

# Rheological Changes During the Drying of a Waterborne Latex Coating

Frank Löfflath—PPG Industries (France) S.A.\*

Matthew Gebhard—Rohm and Haas Co.†

## INTRODUCTION

Rheological changes during drying have a profound effect on final film properties. In particular, these changes affect the ultimate gloss and distinctness of image of the dried film. Rheological changes accompanying drying are due to the effects of evaporation and the concomitant change in dispersion-volume-solids. The rate of evaporation and the relation between viscosity and dispersion-volume-solids have been studied separately but, to our knowledge, there is no work investigating the impact of evaporation on viscosity increases in a drying film comprised of a water-based latex dispersion. Thus, a study of this rather complicated behavior seems appropriate.

From a rheological standpoint, the drying process can be divided into three regions (Figure 1). In the first region, immediately following application, water evaporates at a constant rate and the coating builds viscosity but still behaves as a liquid. At an effective volume fraction of ~65%, the coating enters a second transition region and develops solid-like behavior (yield value). The yield value increases until the film is essentially a solid. In this transition region, polymer particles come into contact, the liquid/air interface is dominated by latex particles, and the rate of water evaporation decreases dramatically. The last stage involves the slow diffusion of solvents out of the film. At this point the film behaves like a solid; however, some creeping flow may take place. The rates at which these processes occur can affect the final film properties, such as flow and leveling, sag resistance, microfoam entrapment, gloss, film formation, mudcracking, and pin holing.<sup>1</sup> In particular, if the coating passes into the second phase very quickly, all of the imperfections introduced during the film application process are frozen in place.

An important aspect of the drying process is water evaporation. Evaporation rates have received much attention<sup>2</sup> over the years. Dillon<sup>2a</sup> derived a very useful mathematical model which includes relative humidity and temperature effects. This model is based on Langmuir-Knudsen<sup>2b,c</sup> and Gardner<sup>2d</sup> treatments of evaporation. While Dillon provides an excellent treat-

*Increases in the low shear viscosity occurring during drying of a water-based latex film were examined as a function of pH, cosolvents, and base. The water and cosolvent evaporation rates were determined as a function of temperature and humidity. Water was found to evaporate with an activity coefficient of 1 and a  $\Delta H_v$  equivalent to pure water. The viscosity changes were determined from a creep measurement. The data is explained by the volume packing model of De Kruif. For several of the films, the ratio between volume and weight fraction was not a static parameter, and an abnormally large drop in the effective volume and weight fraction was observed. This was exaggerated for the samples with ethylene glycol monobutyl ether (EB) or  $\text{NH}_4\text{OH}$ . The high volatility of EB explains the former, while the latter result indicates that  $\text{NH}_4\text{OH}$  suppresses viscosity during drying.*

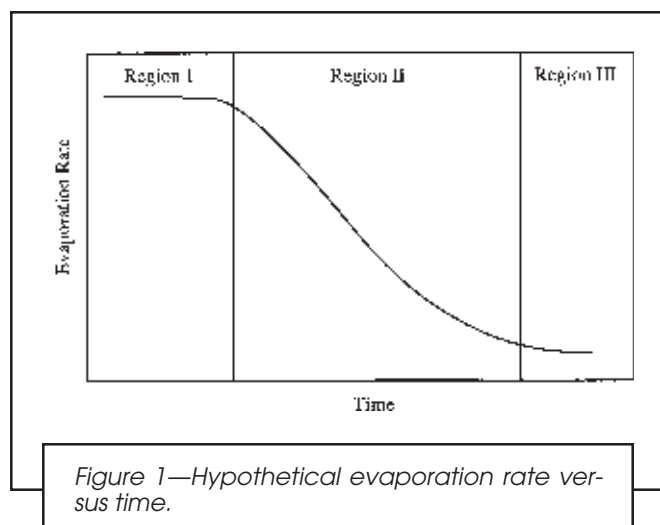
ment for the case of single or mixed solvents, the model does not include effects due to soluble components in the liquid such as salts, surfactants, and cosolvents. These components are present in a water-based latex coating and may impact evaporation; however, there are conflicting reports in the literature<sup>3</sup> on such effects. Thus, a comparison between experimental measurements in water-based latex coatings and existing theories is of interest.

Another crucial aspect of the drying process is the volume-solids effect on viscosity. There have been sev-

Presented at the 69th Annual Meeting of the Federation of Societies for Coatings Technology on October 23, 1996, in Chicago, IL.

\*Route d'Estreux, Boite Postale 6, 59990 Saultain.

†727 Norristown Rd., Spring House, PA 19477.



eral treatments of this, the most notable of which are the theories of Dougherty-Krieger<sup>4</sup> and De Kruif.<sup>5</sup> The theoretical and experimental studies on solvent loss and volume solids effects are very useful and, to a first approximation, it is possible to couple the two effects for a composite theory; however, this strategy overlooks compositional changes in the serum phase which can have an impact on viscosity. Thus, an important question is what effects pH changes, cosolvent evaporation, and increases in salt concentration have on viscosity.

To address these questions, we undertook a study of viscosity changes occurring during drying of two model latex dispersions in which parameters such as starting pH, neutralizing agent, and cosolvents were varied. Water evaporation rates were determined under controlled environmental conditions and evaluated in light of existing theories. This allowed determination of the activity coefficient for water evaporation. Only the viscosity changes of the coatings during the first region of drying were considered. To eliminate complications due to pigments, this study focused on clear coatings. The viscosity was measured in the creep mode using a Carri-Med-CSL 100 controlled stress rheometer. This technique gives the limiting low shear viscosity, thus allowing comparison to the theories<sup>4</sup> relating limiting low shear viscosity to dispersion-volume solids. In addition, the intrinsic viscosity and evaporation rates of the cosolvents were evaluated. Lastly, a dry-time recorder was constructed to measure open-times,\* which were compared to the Carri-Med rheological data.

## THEORETICAL BACKGROUND

### Evaporation Process

There is much work in the literature on measuring evaporation rates of solvents and, in particular, evaporation rates of water from paint films. These studies by Hansen,<sup>6</sup> Sletmoen,<sup>7</sup> and Doolittle<sup>8</sup> employed test methods like the Evapocorder,<sup>9</sup> Evapograph<sup>10</sup> or Evaporometer.<sup>11</sup>

The theoretical basis for much of this work is the kinetic gas theory of Knudsen<sup>2c</sup> and Langmuir.<sup>2b</sup> Knudsen treated the case where the only gas present in the vapor phase is the evaporating solvent. At a temperature,  $T$ , the number of molecules evaporating out of the liquid,  $E_{\max}$ , depends on the surface area,  $A$ , a mass transfer factor,  $k$ , the vapor pressure of the liquid,  $P_v$ , the molecular weight,  $M$ , and the gas constant  $R$ . This is given in equation (1).

$$E_{\max} = kP_v \sqrt{\frac{M}{2\pi RT}} \quad (1)$$

Evaporation in the presence of other gases (e.g., air) is more complicated. Gardner<sup>2d</sup> derived equation (2) for the absolute rate based on diffusion theory.<sup>12</sup>

$$E_L = \frac{KDMP_v}{RTp_x} \quad (2)$$

In equation (2),  $E_L$  is the absolute evaporation rate,  $k$  is a mass transfer constant,  $D$  is the diffusion coefficient of the evaporating gas molecules through the ambient gas,  $p$  is the ambient pressure, and  $x$  is an effective boundary layer film thickness at the liquid surface. If the diffusion coefficient is not known, it can be estimated from the molecular weight and molar volume using Gilliland's equation.<sup>9</sup>

Gilbert<sup>2e</sup> extended the kinetic theory approach to the case where air is present. Not surprisingly, he arrived at an equation for the absolute rate of evaporation in air ( $E_L$ ) similar to the Langmuir-Knudsen equation.

$$E_L = e^{-f} P_v \sqrt{\frac{M}{2\pi RT}} \quad (3)$$

$$f = \frac{S}{Y} \quad (3.1)$$

In this equation,  $f$  is a factor which depends on  $S$ , the height of the stagnant air column above the liquid, and  $Y$ , the mean free path of the molecules in the vapor phase.

A much more useful model is that of Dillon<sup>2a</sup> which includes a treatment for relative humidity. In the Dillon model, the evaporation rate of a given component is assumed to follow first order kinetics with modification for relative humidity.<sup>2e,13</sup> According to Dillon, the evaporation rate is given by equation (4).

$$\frac{dm}{dt} = -AK^{v,T}P_i\sqrt{T}(a - \phi) \quad (4)$$

Here,  $dm/dt$  is the evaporation rate,  $A$  is the surface area,  $K^{v,T}$  is a mass transfer coefficient which depends on air flow and temperature,  $T$  is the absolute temperature,  $p_i$  is the vapor pressure,  $a$  is an activity coefficient, and  $\phi$  is the relative vapor saturation (e.g., relative humidity). Several of the factors in equation (4) are temperature dependent and can be combined in one factor,  $C^{v,T}$ .

$$C^{v,T} = K^{v,T}P_i\sqrt{T} \quad (5)$$

\*In this context the open time is defined as the point where coating flow ceases.

Thus equations (4) and (5) can be rewritten as equation (6). If  $dm/dtA$  is determined at constant temperature and air flow then the activity coefficient of the evaporating solvent can be determined.

$$\frac{dm}{Adt} = -C^{v,T}(a - \phi) \quad (6)$$

The air speed over the surface of the evaporating liquid is a very important factor. In Dillon's treatment, this effect is present in the mass transfer coefficient,  $K^{v,T}$ , as given in equation (7).

$$K^{v,T} = K^0 + \frac{V}{\alpha V + \beta} \quad (7)$$

In this equation,  $V$  is the air speed,  $K^0$  is the mass transfer coefficient in the absence of air flow, and  $\alpha$  and  $\beta$  are the correction factors for air flow which depend on the evaporating liquid; these correction factors are given by Dillon<sup>2a</sup> for several solvents. In actuality, air flow turns out to be the most important parameter for determining absolute rates and, unfortunately, it is the hardest to control or measure.

As can be seen from this model, in order to determine the rate of evaporation, parameters like air speed, temperature, and humidity must be controlled. In addition, film thickness effects must also be considered. Film thickness effects may be important because all of the models described earlier assume that the rate limiting step for evaporation is the transport of the evaporating solvent through the vapor phase and away from the drying film. However, at some point during the drying process, solvent diffusion through the film is the rate limiting step, and the Dillon model is no longer valid. Experience shows<sup>6</sup> that, in the constant evaporation region (I), the rate limiting step is diffusion through the vapor phase, and this assumption can be checked by verifying that the evaporation rates are independent of film thickness.

At constant temperature and air flow, the evaporation rate should be a linear function of humidity [equation (6)]. The slope of the line is  $C^{v,T}$ , and the intercept is a  $C^{v,T}$ . Measurement of these evaporation rates allows the determination of both  $C^{v,T}$  and  $a$ . If  $C^{v,T}$  is determined at constant humidity and air flow and different temperatures, the temperature dependence of  $C^{v,T}$  can be measured. This is given in equation (8), where equation (6) is expanded using the Clausius-Clapeyron equation for vapor pressure, and  $\Delta H$  is the enthalpy of vaporization for the solvent.

$$C^{v,T} = K^{v,T} \sqrt{Te}^{-\frac{k_2}{T}} \quad (8)$$

$$k_2 = \frac{\Delta H}{R} \quad (8b)$$

The effect of temperature on the mass transfer coefficient,  $K^{v,T}$ , is assumed to be constant.

### Viscosity and Volume Fraction

As with evaporation rates, there are several excellent treatments of the viscosity dependence on volume frac-

tion of a dispersion. At dilute concentrations ( $< \sim 5\%$  volume solids) the viscosity of a latex suspension depends only on the volume fraction. Factors such as interparticle forces are unimportant. A theoretical treatment [equations (9) and (10)] for the viscosity in this regime was derived by Einstein and has since been verified using synthetic mono-disperse particles.<sup>14</sup>

$$\eta = \eta_0(1 + 2.5\phi) \quad (9)$$

$$\eta_r = \frac{\eta}{\eta_0} \quad (10)$$

In this equation,  $\eta$  is the viscosity of the suspension,  $\eta_0$  is the viscosity of the medium,  $\eta_r$  is the relative viscosity, and  $\phi$  is the volume fraction of latexes. The resulting equation is useful because it is independent of the latex size. Deviations from equation (9) can occur in situations where flocculation or agglomeration exist; however, such deviations are evident in a nonlinear viscosity dependence on  $\phi$ .

As the volume fraction of latexes is increased, significant deviation from equation (9) occurs. In particular, the viscosity increases rapidly as  $\phi$  increases. A very useful treatment [equation (11)] is the model given by Dougherty and Krieger,<sup>11</sup> where  $p_k$  is the volume packing fraction, and  $[\eta]$  is the intrinsic viscosity.

$$\eta_r = \left[ 1 - \frac{\phi}{p_k} \right]^{-[\eta]p_k} \quad (11)$$

There is much debate about the value of these parameters, and they are known to be dependent upon the shear rate. A useful equation is the very low shear rate limit as derived by De Kruif [equation (12)]. Equation (12) predicts that at a volume fraction of 0.63 the viscosity at low shear goes to infinity.

$$\eta_r = \left[ 1 - \frac{\phi}{0.63} \right]^{-2} \quad (12)$$

Equations (9-12) are very useful for predicting the viscosity of latex suspensions; however, they are all given in terms of latex volume fraction. This presents a problem because volume fractions are ill defined and, in practice, only the weight fraction is known. Therefore, equations (9-12) are most useful for determining effective volume fractions at high concentrations. An important parameter then becomes the ratio of the volume ( $\phi_v$ ) to the weight fraction ( $\phi_m$ ).

$$v_f = \frac{\phi_v}{\phi_m} \quad (13)$$

If equation (13) is inserted into equation (9) the result is equation (14).

$$\eta_r = (1 + 2.5V_f^1\phi_m) \quad (14)$$

Thus, the intrinsic viscosity can be used to determine the effective hydrodynamic volume,  $V_f^1\phi_m$ , of the latex at low volume fractions. In practice,  $V_f^1 > 1$  for an acrylic latex ( $\rho \approx 1.1 \text{ g/cm}^3$ ). This is due to physical swelling of

Table 1—Physical Parameters of Latexes Used in this Study

Physical Parameters	Latex A	Latex B
Composition (wt%)	64% BA/31%MMA/5%MAA	38%BA/57%MMA/5%MAA
Solid content as supplied	41.4%	42.6%
Particle size	95 nm	95 nm
T <sub>g</sub> <sup>b</sup>	0°C	50°C

(a) As measured with a Brookhaven BI-90, Brookhaven Instruments Corp., Ronkonkoma, NY.  
(b) Calculated using the Fox equation<sup>17</sup>

the latex and electric double layer contributions. Determination of  $V_f^1$  allows an assessment of the effective volume fraction in the dilute regime. It is also indicative of the volume fraction present at the beginning of the drying process for a latex film.

By combining equation (12) and equation (13) the result is equation (15).

$$\eta r = [1 - V_f(t)\phi_m/0.63]^{-2} \tag{15}$$

Therefore, the viscosity during drying is not only a function of the weight fraction, but it is also a function of the time dependent  $V_f$  factor. During the drying of a latex film, several events cause the  $V_f$  factor to change. Due to physical swelling of the latex by cosolvents and base and to electric double layer effects which arise from the anionic charge, the effective volume fraction of a typical anionic water-based latex dispersion may be anywhere from 10% to several times larger than its weight fraction. In addition, the electric double layer is affected by the ionic strength of the formulation. Thus, the nature and amount of cosolvents used in the formulation influence the  $V_f$  factor, as will the amount and type of base and changes in the ionic strength. During the drying process, cosolvents and ammonia evaporate from the drying film and the ionic strength typically increases, causing a decrease in  $V_f$ . It is the magnitude of these effects which we tried to characterize in the work presented here. If equation (15) is used to fit the viscosity versus weight % solids data then the  $V_f$  factor at the instant that the coating develops an infinite low shear viscosity ( $V_f^h$ ) is determined. In this context,  $V_f^h\phi_m = 0.63$  at the point that an infinite low shear viscosity is achieved.

Combination of Evaporation and Volume-Fraction/Viscosity Equations

During the early drying stages of a latex film, the rate of water evaporation is assumed to be constant. In light of this assumption, the weight fraction at time  $t$ ,  $\phi_m$ , is given by equation (16).

$$\phi_m = \frac{\phi_m(t=0)}{(1-E't)} \tag{16}$$

$$E' = \frac{E}{m(t=0)} \tag{16b}$$

In this equation,  $E$  is the absolute rate of solvent evaporation (g/min),  $E'$  is the relative rate of evaporation (1/min),  $\phi_m(t=0)$  is the initial weight fraction, and  $m$  is the initial mass of the film. Combining equation (16a) with equation (15) gives equation (17), which gives the time dependence of the viscosity in terms of the parameters  $\eta_0$ ,  $V_f$ ,  $\phi_m(t=0)$ , and  $E'$ . In practice,  $\phi_m(t=0)$ , and  $E'$  are known and the viscosity data are used to determine  $V_f$  and  $\eta_0$ .

$$\eta_r = \left[1 - \frac{V_f}{0.63} \left( \frac{\phi_m(t=0)}{1-E't} \right) \right]^{-2} \tag{17}$$

$E'$  is a particularly useful parameter because it allows data collected at different evaporation rates and film thicknesses to be compared. In principle, the viscosity versus time data is confounded by differences in absolute evaporation rates, making comparison between dif-

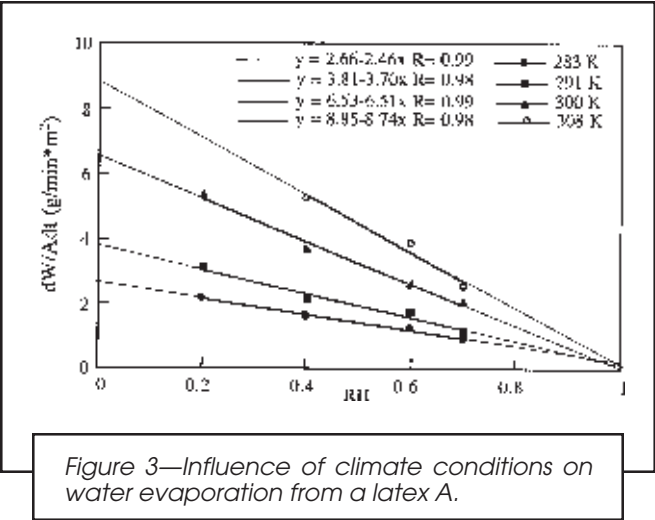
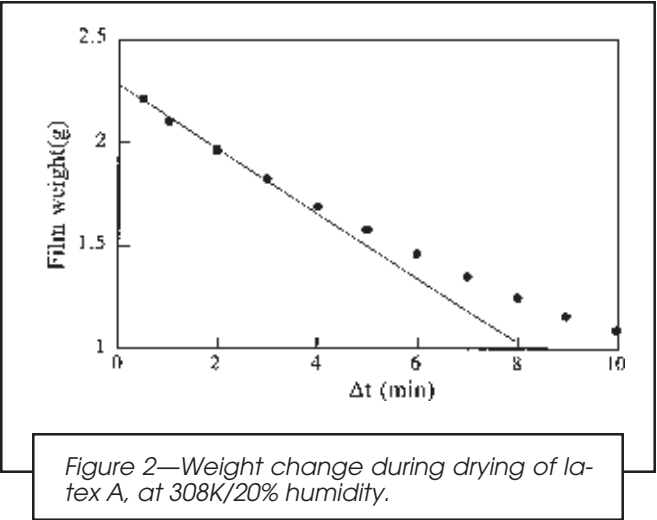




Table 2—Evaporation Rates Measured at 300K/40% Humidity, Air Flow (0.5m/sec)

## 1. Influence of film thickness: Latex A, pH 7.5

Film thickness ( $\mu\text{m}$ )	Evaporation Rate (g/min)* $10^{-1}$	Evaporation Rate Per Unit Area (g/min/cm <sup>2</sup> )* $10^{-4}$
40 .....	1.10	4.07
50 .....	1.09	4.04
90 .....	1.12	4.15
150 .....	1.12	4.15

2. Influence of pH: Latex A, (80 $\mu\text{m}$ )

Base/pH	Evaporation Rate (g/min)* $10^{-1}$	Evaporation Rate Per Unit Area (g/min/cm <sup>2</sup> )* $10^{-4}$
NH <sub>4</sub> OH/pH 8.5 .....	1.11	4.11
NH <sub>4</sub> OH/pH 9.5 .....	1.08	4.00
NaOH/pH 9.5 .....	1.10	4.07

3. Influence of cosolvents: Latex B, (80 $\mu\text{m}$ ), pH 8/NH<sub>4</sub>OH

Latex B + cosolvent	Evaporation Rate (g/min)* $10^{-1}$	Evaporation Rate Per Unit Area (g/min/cm <sup>2</sup> )* $10^{-4}$
neat Latex B .....	1.10	4.07
Latex B + EB .....	1.09	4.04
Latex B + DB .....	1.10	4.07
Latex B + PNB .....	1.09	4.04
Latex B + DPnB .....	1.10	4.07
Latex B + DM .....	1.09	4.04
Latex B + DPM .....	1.11	4.11

ferent samples impossible; however, by comparing data as a function of  $E't$  this complication can be avoided.  $E't$  is the relative amount of solvent that has left the film, and is independent of absolute evaporation rate, time, and film thickness.

To check reproducibility, evaporation rates were determined at the same temperature and humidity on 10 different days. An analysis of the results indicated that the experimental error was about 8.5% which is reasonable considering the potential sources of error such as air flow and temperature-humidity fluctuations.

## EXPERIMENTAL DATA

## Raw Material and Sample Preparation

The measurements of viscosities were performed on two model acrylic latexes (Table 1). Both latexes were made by standard polymerization procedures employing a thermal, persulfate-initiated semi-continuous monomer emulsion addition process; methacrylic acid and one percent sodium dodecyl benzenesulfonate (based on monomer) were used to stabilize the latexes.

## Evaporation Measurements

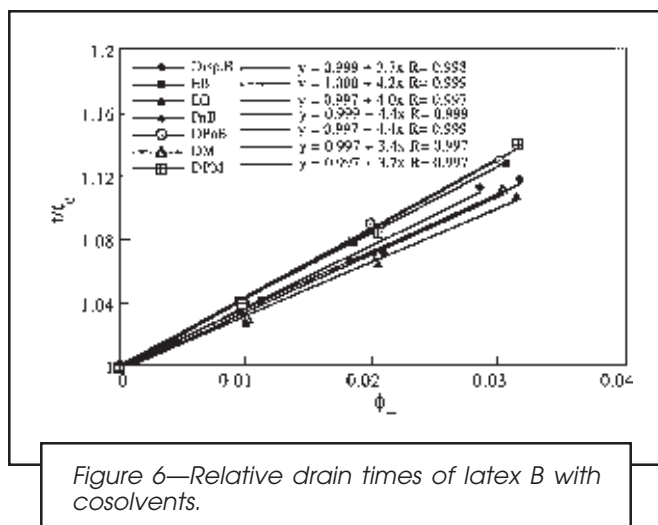
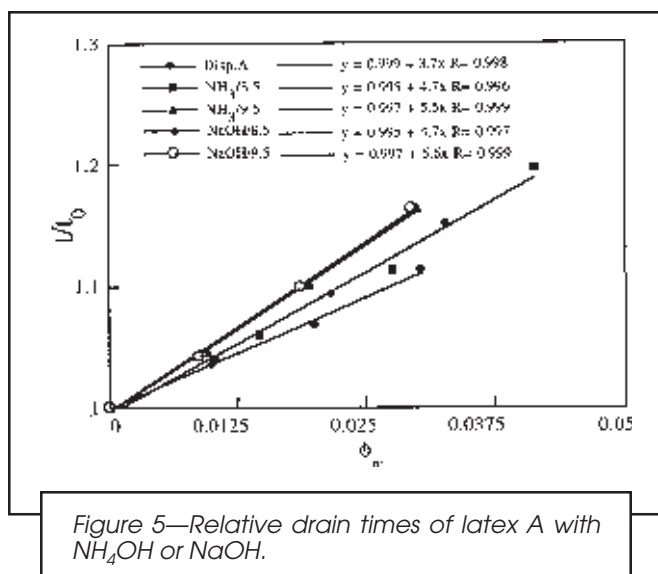
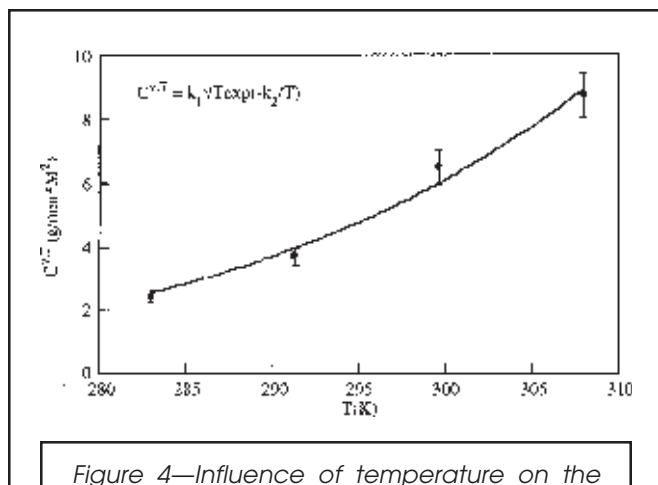
Evaporation rates (i.e., weight loss as a function of time) were determined at several temperatures and relative humidities. In addition, the effects of film thickness, initial pH, neutralizing base, and cosolvents on evaporation rates were determined. The samples were drawn down over a glass plate at a film thickness of 180  $\mu\text{m}$  and a total area of 270  $\text{cm}^2$ . The temperature and humidity which varied by  $\pm 5\%$ , were determined by a sling psychrometer, model WE 1330P (Gardner). Air flow was kept relatively constant using a box to shield the samples from stray drafts, and was determined using an Anemometer, Model Velometer Jr. range (0-10) m/sec (Gardner).

## Viscosity Increase During Evaporation

**Sample Preparation:** Samples of latex A were prepared at pH values of 8.5 and 9.5 using NH<sub>4</sub>OH or NaOH as the neutralizing agent. In addition, latex A was used as supplied at pH 7.3. During the synthesis of latex A and B, NH<sub>4</sub>OH was added as the neutralizing agent for stability. Thus, the control experiment with latex A at pH 7.3 was actually carried out with NH<sub>4</sub>OH as the neutralizing agent. Latex B was prepared with 20% cosolvent (Dowanol™ EB, DB, PnB, DPnB, DM, and DPM)\* based on polymer solids. The pH of the samples was adjusted to 8.0 using NH<sub>4</sub>OH.

These samples were drawn down over a glass panel at a film thickness of 180  $\mu\text{m}$ . This was done in a controlled environmental room at constant temperature (298 $\pm$ 2K) and humidity (50 $\pm$ 5%). The air flow was controlled using a box to shelter the panels from stray breezes. A small fan was placed in the back of the box to generate a small but relatively constant air flow. At set time intervals, the samples were removed from the panel using a rubber squeegee. The time intervals were chosen based on the observed open time. Typically five viscosity/time data points were obtained for each sample.

\*Dowanol is a trademark of the Dow Chemical Company, EB—ethylene glycol monobutyl Ether, DB—diethylene glycol monobutyl ether, DM—diethylene glycol monomethyl ether, PnB—propylene glycol monobutyl ether, DPnB—dipropylene glycol monobutyl Ether, DPM - dipropylene glycol monomethyl ether.



Prior to viscosity measurement, all the samples were filtered to remove any dried polymer which could become lodged between the cone and plate of the rheometer.

**Viscosity Measurements:** The previously mentioned models for viscosity are valid in the low shear rate limit. Therefore, in order to get data which can be used in these models, a very low shear measurement is required. By far, the best way to extract the data is through a creep measurement. In this experiment a constant and low stress is applied and the amount of deformation [compliance (J)] is measured. The viscosity is given by the reciprocal of the rate of compliance ( $dt/dJ$ ).

Viscosity was determined using the Carri-Med CSL 100 controlled-stress cone and plate rheometer, with a 6 cm diameter  $2^\circ$  cone at a stress of 0.1 Pa at  $20^\circ\text{C}$ . The data was obtained as compliance versus time. All the samples were presheared at 15 Pa for 30 sec and allowed to equilibrate for one minute prior to the creep measurement. The rheometer was calibrated using a standard oil. Data is only presented for those samples which did not display an elastic component.

**Additional Sample Data:** In addition to measuring viscosity, the pH, cosolvent levels, and weight solids were also determined. The solid content was measured by drying the samples for 24 hr at  $120^\circ\text{C}$ . pH was measured with the Corning 240 pH meter. Also, the effect of pH and neutralizing agent on the viscosity of latex A was determined at 35% weight solids. The cosolvent level in the samples was determined using the gas chromatograph Model 5890 from Hewlett Packard, with a flame ionization detector. The determinations were done in THF, and compared against known standards.

### Intrinsic Viscosity

The measurement of intrinsic viscosity of a latex is complicated by salt effects on the electric double layer. To perform the experiment, samples need to be diluted to low solids ( $< 5\%$ ); however, if deionized water is used, the serum composition changes dramatically, impacting the intrinsic viscosity. To circumvent this problem, a sample of the serum phase of each of the formulations was isolated using ultrafiltration. The samples were first prepared with the desired cosolvent and base neutralization and allowed to equilibrate for 24 hr. The serum was isolated using an Amicon Model 8200 ultrafiltration cell. The membrane had a 300,000  $M_w$  cutoff, which at 1 g/cm corresponds to a 5 nm pore size. The back pressure was 5 psi. The use of a low back pressure keeps the filter from clogging. This serum was then used to dilute the latex formulations back to the desired concentration.

The viscosities at 0, 1, 2, and 3% solids by weight were determined using a capillary viscometer at  $25^\circ\text{C}$  in a water bath, controlled by a thermostat (VWR, Model 1110). This technique provides drain times for each sample; however, since these times are proportional to the kinematic viscosity and we are only concerned with relative viscosities, no further attempt was made to convert these times into viscosities. The relative drain time,

Table 3— $V_f^1$  from Intrinsic Viscosity and Fits to Equation (15)

Sample	$V_f^1$	$V_f^1/\text{Latex A or B}$	$V_f^h$	$V_f^h/\text{Latex A or B}$
Neat Latex A .....	1.47	1.00	1.36	1.00
Latex A + $\text{NH}_4\text{OH}$ to pH 8.5 .....	1.87	1.27	1.33	0.978
Latex A + $\text{NH}_4\text{OH}$ to pH 9.5 .....	2.20	1.50	1.29	0.949
Latex A + NaOH to pH 8.5 .....	1.87	1.27	1.34	0.985
Latex A + NaOH to pH 9.5 .....	2.23	1.52	1.41	1.04
Neat Latex B .....	1.46	1.00	1.33	1.00
Latex B + EB .....	1.68	1.15	1.24	0.932
Latex B + DB .....	1.58	1.08	1.34	1.01
Latex B + PnB .....	1.76	1.21	1.39	1.05
Latex B + DPnB .....	1.77	1.21	1.53	1.15
Latex B + DM .....	1.37	0.983	1.31	0.985
Latex B + DPM .....	1.48	1.01	1.37	1.03

$t/t_0$ , should be a linear function of  $\phi_v$ , and should have a slope of 2.5. Deviations of the slope from 2.5 give the  $V_f^1$  factor discussed in the theoretical section.

### Determination of Open Time

The cessation of flow of the liquid is an important physical phenomenon during the drying of a latex. In this context, open time ( $t$ ) is defined as the time between application and cessation of flow. In order to compare data generated under different film thickness and environmental conditions it is necessary to determine the dimensionless parameter  $E't$  (i.e., the relative amount of water that has left the film). Based on equation (17), flow ceases in the low shear rate region at a given  $E't$ . In order to determine the open time for each of the samples, a dry time recorder was used. The majority of commercial dry time recorders are designed to track the drying of alkyd paints and thus are much too slow for this application. Therefore, a suitable dry time recorder was constructed. For this test a stylus is dragged through the film at  $\sim 2.5$ – $5$  cm/min. As long as the coating is fluid it flows back and no mark is left. Once the open time is reached, the coating stops flowing and a permanent mark is left. The distance the stylus traveled without leaving a mark gives the time.

The measurements were done at 300 K, 40% humidity, an air speed of 0.5 m/s, and a film thickness of  $80 \pm 5$   $\mu\text{m}$ . The stylus speed was 3.8 cm/min. The glass panel was weighed immediately after application to get an actual film thickness. In addition, the relative evaporation rate was determined ( $E'$ ), allowing the dimensionless open time to be determined.

## RESULT AND ANALYSIS

### Evaporation Rates

A typical weight loss versus evaporation time is given for latex A in Figure 2. The data is for the sample dried at 308 K, and 20% RH. The data shows that even at fairly long times the weight loss remains constant. As a reference, the open time of this sample under these conditions was about two minutes. This means that for the purposes of the experiments presented here, the evaporation rate is constant.

The data at different temperatures are plotted versus relative humidity (RH) in Figure 3, and a straight line is fit at each temperature. The fits were not constrained to 0 at 100% RH. From the slope and intercept, the activity coefficients were all within experimental error ( $\sim 10\%$ ) of being 1. Thus, during the early stages of drying the water is evaporating as if it was pure water. This result is consistent with those of Hansen.<sup>15</sup>

As set forth in the theoretical section, the slope of the lines gives the maximum evaporation rate which is dependent on temperature among other things. The temperature dependent  $C_v^T$  values are shown in Figure 4, along with a fit to equation (8). To within the error of the measurements, the measured  $\Delta H_v$  is equivalent to pure water.

These results indicate that at least during the early stages of drying the temperature and humidity dependence of the evaporation of water is completely unaffected by the presence of the latex. This result is consistent with results obtained by Pramoganey<sup>16</sup> and Kornum.<sup>3g</sup> However, the results do not address the fact that the latex may reduce the absolute rate by affecting the effective evaporative surface area. Additional results on samples at different film thickness, different starting pH values, and in the presence of cosolvent (Table 2) reveal the surprising result that none of these components have an effect on the evaporation rate. In other words, in the early stages of drying, the evaporation of water from a latex film depends on temperature, air flow, and humidity.

### Intrinsic Viscosity

The relative drain times for the samples prepared from latex A or latex B are plotted in Figures 5 and 6, respectively. The best fit of a line through the points is also provided. Using the Einstein relation, the correction factors,  $V_f^1$ , were determined (Table 3). As a reference, all of the  $V_f^1$  factors were divided by the value obtained for the neat latex (column 3).

As expected, samples at high pH display the greatest volume increase and little difference is noted between  $\text{NH}_4\text{OH}$  and NaOH. Thus, the degree to which each of these bases swell the latex is quite similar. Also, the cosolvents elicited varying degrees of latex swelling, in accord with their relative hydrophobic or hydrophilic

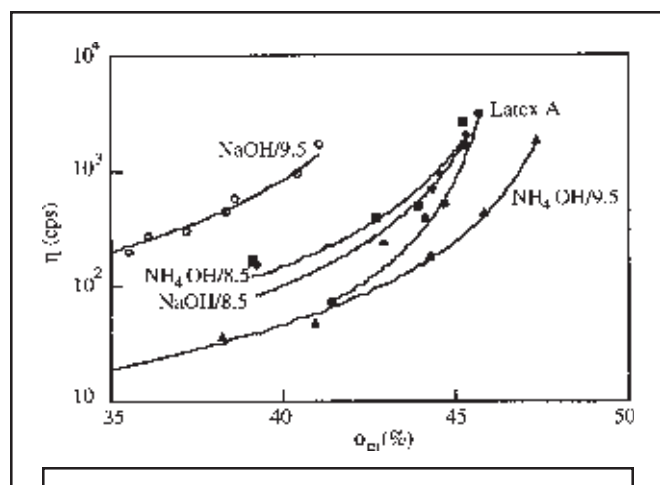


Figure 7—Viscosity versus weight solids content for Latex A with  $\text{NH}_4\text{OH}$  or  $\text{NaOH}$ .

character. The two hydrophobic cosolvents (PnB and DPnB) were found to swell latex B the most. EB and DB give the intermediate swelling and are known to only partially partition into the latex. Lastly both DPM and DM cause little swelling and are expected to predominantly remain in the water phase.

Based on the intrinsic viscosity data, the assumption that the  $V_f$  factors determined remain constant during the drying process, and the assumption that the volume fraction at which gelation occurs (infinite low shear viscosity) is a fixed value ( $\phi = 0.63$ ); the samples with the highest pH are expected to display gelation at the lowest weight percent. There would also be no difference between  $\text{NH}_4\text{OH}$  and  $\text{NaOH}$ . A similar statement could be made for the samples containing PnB and DPnB. If a comparison is made between samples at the same initial starting weight percent solids, this data would indicate that high pH and PnB or DPnB gives the shortest open time. However, as shown in the following, this is based on the invalid assumption that the  $V_f$  factor is constant during the drying process.

### Viscosity Increase During Drying

The wt% solids versus viscosity data is plotted in Figures 7 and 8. A useful and simple way of interpreting the data is estimated, based on the shape of the curve, at what wt% solids the viscosity becomes infinite. For example, latex A neutralized to pH 9.5 with  $\text{NaOH}$  has a much higher viscosity at a given solids than the control sample (Latex A with no added base). This difference is present throughout the drying process, and amounts to a shift to the left in the wt% solids versus viscosity curve. Curves which lie to the left of the control indicate that the ratio between the volume and weight fractions ( $V_f$ ) is larger than the control, and this condition persists throughout the drying process. Curves which lie to the right of the control indicate that  $V_f$  is smaller than the control, or at least that at some point during the drying process,  $V_f$  becomes smaller. It is important to remember that during the drying process  $V_f$  is a dynamic parameter, and that only relative comparisons are valid

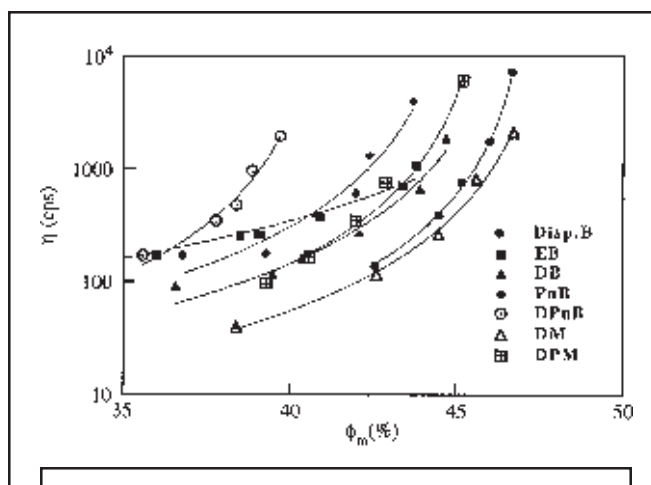


Figure 8—Viscosity versus weight solids content for latex B with cosolvents.

(i.e., Latex A with different bases and different pH values).

As expected, the viscosity is much higher at a given wt% solids for the high pH sample containing  $\text{NaOH}$  (Figure 7,  $\text{NaOH}/9.5$ ). However, the data for the pH 9.5 sample with  $\text{NH}_4\text{OH}$  reveals a much lower viscosity at a given wt% solids. In fact, it is seen that this sample has a lower viscosity than even the control sample (latex A initially at pH 7.3). Versus the latex A control, the presence of the added  $\text{NH}_4\text{OH}$  to latex A allows the sample to achieve a significantly higher wt% solids during drying, before reaching an infinite viscosity. This is completely counterintuitive, especially since the measurement of the final pH of the samples reveals that the sample starting at pH 9.5 winds up at pH 7.9, while the control sample at pH 7.3 winds up at pH 7.1.

In general, as the pH is raised through addition of a base like  $\text{NH}_4\text{OH}$ , the viscosity will increase due to a neutralization of carboxylic acid groups and a concomitant swelling of the latex; however, the viscosity/%wt solids data provided earlier indicates that it is possible to prepare a sample that has a higher pH, a higher wt% solids, and yet a significantly lower viscosity. This means that the route by which the sample is prepared can impact the viscosity. The act of adding  $\text{NH}_4\text{OH}$  to latex A, then allowing water and  $\text{NH}_3$  to evaporate during drying brings the system to a different state than if water was first removed from the latex and then  $\text{NH}_4\text{OH}$  was added to bring the pH to 7.9.

The data for the cosolvent series also reveals some interesting trends. In general, the addition of a cosolvent to latex B causes it to develop an infinite viscosity at lower wt% solids than for the control sample (latex B with no cosolvents); however, some solvents actually suppress viscosity during drying.

DPnB causes latex B to develop an infinite viscosity at the lowest wt% solids. This is expected based on the hydrophobic low-volatility nature of DPnB. Because of the low solubility of DPnB in water, an overwhelming fraction of DPnB partitions into the latex particle. This causes a physical swelling of the latex and an increase in



the effective volume fraction occupied by the latex and an increase in the viscosity. Because of the low volatility of DPnB, virtually none of it evaporates during the time scale of the drying process studied here.

Interestingly, PnB, like DPnB, has a low water solubility and also swells the latex significantly; however, it has a much higher evaporation rate, and thus the PnB can evaporate during drying. At the beginning of the drying process both the sample with PnB and the sample with DPnB have very similar viscosities at the same wt% solids. This indicates that both PnB and DPnB initially swell latex B to the same extent; however, the volatilization of PnB during drying leads to a reduction in effective volume fraction, and a shift in the wt% solids/viscosity curve to higher weight fractions relative to DPnB, as evidenced in Figure 8 (DPnB versus PnB).

DB and DPM are both completely miscible in water, but they also partition into the latex, and cause an increase in the effective volume fraction and the viscosity. As expected, this causes a shift relative to the control in the wt% solids/viscosity curve to lower wt% solids. When compared to DPnB and PnB, this shift is not as large, and can be explained based on the incomplete partitioning into the latex. This partitioning effect is also seen in the intrinsic viscosity data ( $V_f^1$  in Table 3). During the time scale of the drying process studied here, neither DB or DPM are volatile enough to leave the coating in any significant amount.

While most of the cosolvents in the series cause an increase in viscosity upon addition, the addition of DM to latex B actually causes a drop in viscosity and this translates into lowered viscosity throughout the drying process. DM is so hydrophilic that it does not partition into the latex and, in fact, it tends to cause the latex to shrink slightly. This effect is also seen in the intrinsic viscosity data ( $V_f^1$  in Table 3). By virtue of this shrinking effect, a shift to the right is seen in the wt% solids/viscosity curve. It should be noted that DM does not evaporate significantly during the time scale of the drying process studied here.

The effect of EB on the viscosity is quite unique among these cosolvents. Although it is completely water miscible, a significant fraction partitions into the latex, initially increasing the effective volume fraction and the viscosity. However, the high volatility of EB causes it to evaporate from the film at a rate comparable to the evaporation of water, and the effective volume of the EB swollen latex is decreasing during the drying process. This effect translates into lower viscosities later in the drying process, such that the sample, when compared to the control, can achieve a higher weight % solids before reaching an infinite viscosity. At high volume fractions EB appears to have an effect not unlike that of DM. It is also very interesting to compare the behavior of EB with that of PnB. Both have comparably high volatilities, but very different behaviors during drying. A possible explanation is that the PnB is trapped in the latex and its ability to evaporate is significantly reduced, while on the other hand EB, by virtue of its miscibility with water, can more easily evaporate.

A useful way of comparing the data is through the  $V_f^h$  factors, and these are given in Table 3. The  $V_f^h$  factor was

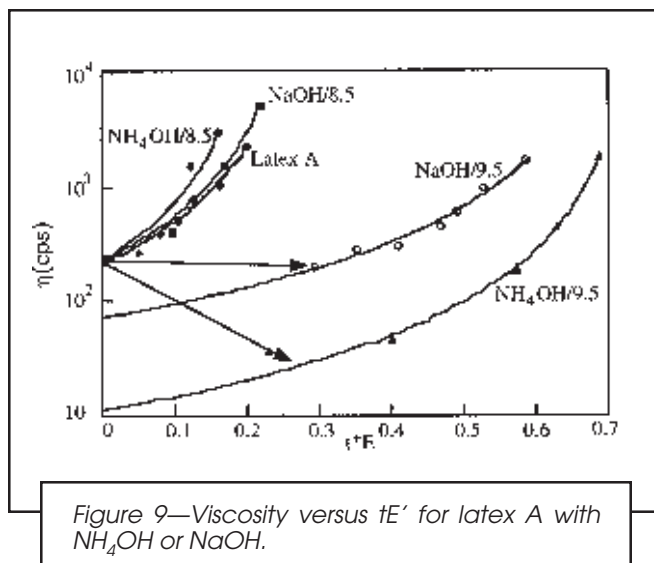


Figure 9—Viscosity versus  $tE'$  for latex A with  $\text{NH}_4\text{OH}$  or  $\text{NaOH}$ .

obtained by fitting the viscosity versus wt% solids data (Figures 7 and 8) to equation (15). The fits were performed by letting both the zero point viscosity [ $\eta_r(\phi_m=0)$ ] and the  $V_f^h$  factor float as free parameters. The  $V_f^h$  factor, as defined in the theoretical section, is the ratio of the volume to weight fraction at the instant that the coating develops an infinite low shear viscosity (i.e.,  $V_f^h\phi_m = 0.63$ , when  $\eta_r = \infty$ ). Column 4 gives  $V_f^h$ , and column 5 gives  $V_f^h$  relative to the control. A quick scan of column 5 reveals that several of the factors are less than one, and of particular note are the materials which give the lowest factors:  $\text{NH}_4\text{OH}$  pH 9.5, and EB.

Another useful comparison between the drying curves comes from adjusting the data so that all the samples start at the same initial viscosity. This amounts to a minor shift along the time axes for the curves. To facilitate the comparison, the data must be plotted as a function of  $E't$  for the reasons discussed previously. The data are plotted in Figures 9 and 10. When plotted in this way the high initial pH samples stand out as being significantly different from the other samples; however, it should be remembered that the starting solids of the

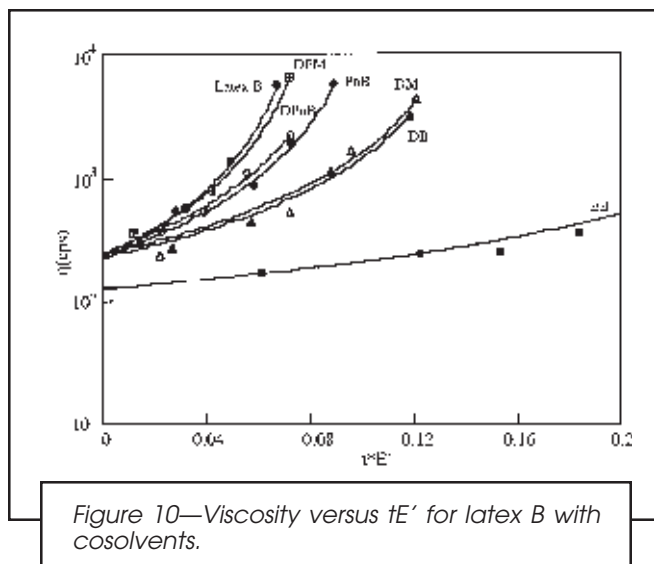


Figure 10—Viscosity versus  $tE'$  for latex B with cosolvents.

Table 4—Percentage of Cosolvent Remaining in the Film

EB	† (min) %C BOP1	0 18.8	2 16.0	4 15.6	6 14.8	7 14.5	8 13.9
DB	† (min) %C BOP	0 21.3	2 21.7	3 22.3	4 20.8	5 21.8	6 23.0
PnB	† (min) %C BOP	0 22.6	2 19.9	3 19.9	4 19	4.5 18.1	5 16.1
DPhB	† (min) %C BOP	0 26.4	1 22.9	1.5 21.9	2 21.6	2.5 20.6	
DM	† (min) %C BOP	0 21.0	3 21.3	5 21.7	6 21.0	7 20.8	21.7
DPM	† (min) %C BOP	0 19.8	1 20.8	2 20.5	3 18.6	4 21.4	

(1) Percentage of cosolvent based on polymer

NaOH sample are much lower. The plots for the cosolvent series also show that EB provides a significant effect on the development of the viscosity. Thus, open time is significantly extended for samples which contain EB.

### Physical Changes in the Sample Upon Drying

The data previously mentioned clearly shows that during the drying process, the amount of swelling ( $V_f$ ) is a dynamic variable and changes significantly. The two effects contributing to this change are evaporation of cosolvents (latex B) and  $\text{NH}_4\text{OH}$ . Data were obtained for both of these effects and can give some insight into their origin.

**Cosolvent Evaporation:** The amount of cosolvent left in the samples at the various dry times was determined by GC. This data is given in Table 4 in terms of percent cosolvent based on polymer solids in the film. As expected, the highly volatile EB and PnB, show a decrease in level as the drying proceeds. This data explains why the  $V_f$  factors, for both EB and PnB are changing during the drying process. For all of the other cosolvents, the level is seen to remain constant when compared to experimental error.

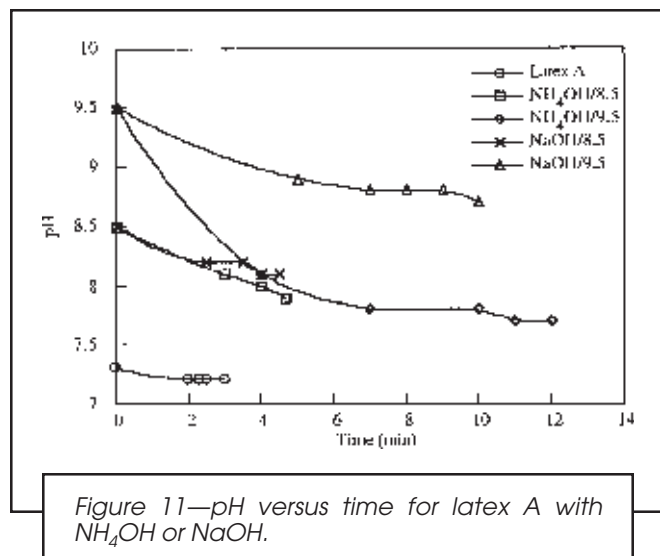


Figure 11—pH versus time for latex A with  $\text{NH}_4\text{OH}$  or NaOH.

### pH Changes and the Effect of $\text{NH}_4\text{OH}$ on Viscosity:

The pH of latex A with added  $\text{NH}_4\text{OH}$  or NaOH is plotted versus drying time in Figure 11. All of the samples show a drop in pH in the first few minutes during the drying process. Even the samples neutralized with NaOH show a decrease in pH. At first, this may seem a little odd until it is remembered that all of the samples contain some  $\text{NH}_4\text{OH}$  which was carried along from the synthesis of the latex. Evaporation of  $\text{NH}_3$  could explain this pH drop. The adsorption of atmospheric  $\text{CO}_2$  could also be playing a role. Interestingly, the sample which starts at pH 9.5 with  $\text{NH}_4\text{OH}$  drops quickly in pH such that within 3-4 min it is at the same pH as the sample that started at pH 8.5.

Figure 12 shows that pH dependence of the viscosity of latex A at constant wt% solids. The viscosity of latex A is highly dependent on pH, showing a rapid rise between pH 8 and 9. Also, the increase is much more significant for the NaOH sample, and while the NaOH sample plateaus at pH 9.5, the sample with  $\text{NH}_4\text{OH}$  drops in viscosity as the pH is increased above 9.5. The viscosity decrease indicates that the presence of  $\text{NH}_4\text{OH}$  suppresses viscosity. A separate titration of latex A reveals that at pH, 9.5, 97% of the polymer acid is ionized. This is consistent with the plateau observed in the NaOH viscosity data.

One possible explanation is that the  $\text{Na}^+$  ions contribute to latex swelling more than  $\text{NH}_4^+$ ; however, the intrinsic viscosity data indicates that at low solids the swelling of latex A is the same for both NaOH and  $\text{NH}_4\text{OH}$ . Taken together, these results indicate that  $\text{NH}_4\text{OH}$  somehow reduces the interaction between the latex particles at high volume solids. The most plausible reason for this viscosity reduction is the effect that  $\text{NH}_4^+$  ions have on shielding the charge on the latex, causing a reduction in viscosity. Another important consideration is the differences in molar equivalents of the two bases needed to achieve a given pH.

This data gives insight into the origin of the  $\text{NH}_4\text{OH}$  behavior. An important effect is the drop in pH which causes a large viscosity drop in the initial drying stages. In the first few moments during the drying process, the pH drops and the system resembles the lower initial pH sample, but with a lower weight-solids and a lower

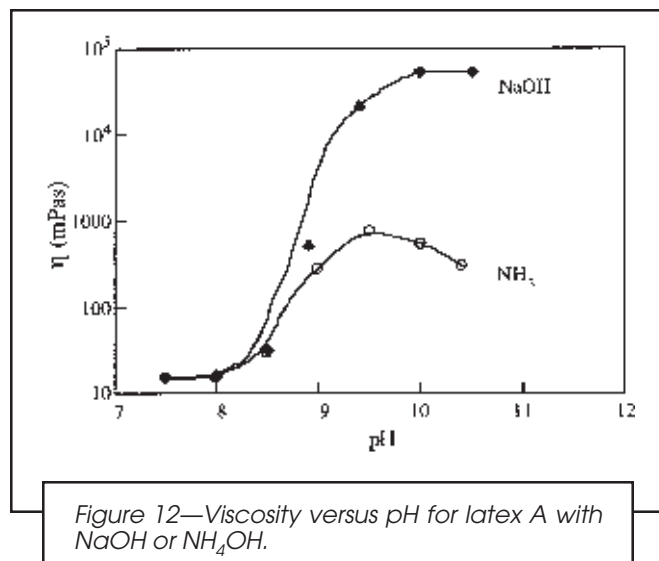


Figure 12—Viscosity versus pH for latex A with NaOH or  $\text{NH}_4\text{OH}$ .

viscosity. Additionally, the presence of the initial  $\text{NH}_4\text{OH}$  suppresses the viscosity, allowing it to achieve a significantly higher solids before cessation of flow.

### Correlation Between Drying Curve Data and Open-Time

Throughout this paper it is assumed that there is a correlation between the rheology changes that occur during the drying of a latex film and the open time. In addition, it is assumed that the rheological changes which occur for the film can be understood in terms of a particle packing model. Implicit in this last assumption is the belief that the latex film dries uniformly from top to bottom (i.e., skinning is not important) and from edge to center.

A pragmatic test of these assumptions is the existence of a correlation between the point of infinite viscosity as determined from the drying curves, and the open time as measured with the dry time recorder. If these two values are correlated, then at the very least, the physical model is consistent with observations, and the D-K model and the drying rate model can be combined to predict relative trends in the open time. Lastly, if air flow rate can be kept constant, it allows open time data obtained at different temperatures and RH to be directly compared.

To test this assumption, the open time was measured for the same series of samples used for the drying study. Open time is given in terms of the dimensionless parameters  $E't$ . Figure 13 gives a plot of the dimensionless open time versus the time to reach infinite viscosity as predicted by equation (15), and a reasonably good correlation is observed.

## DISCUSSION

This work shows that the rates of evaporation from a latex, as well as the accompanying rheological changes can be measured with uncomplicated and practical methods. The Dillon model can be used to determine the

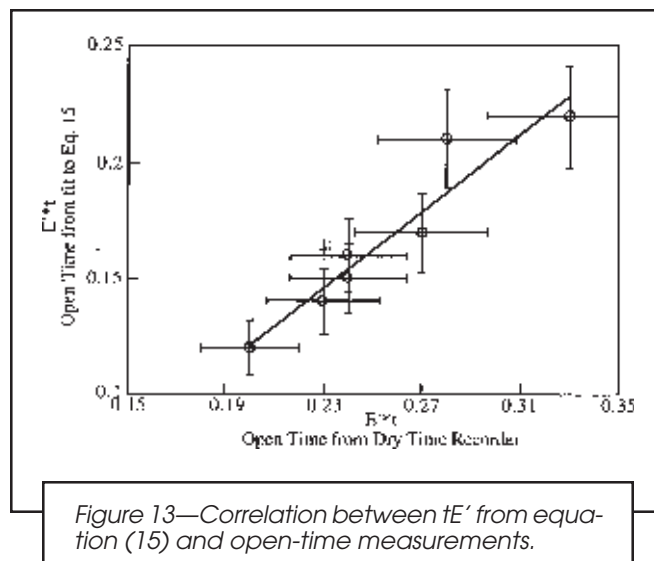


Figure 13—Correlation between  $E't$  from equation (15) and open-time measurements.

effects of temperature and humidity on the drying process. In the early stages of drying the water can be assumed to evaporate from a latex as if it were pure water. This result is extremely useful in that many of the complicating factors can be ignored. In addition, the Dougherty-Krieger and De Kruif models were found to give a physical understanding for the viscosity increase. These two models could be combined to give an expression for the time evolution of the viscosity as a function of the dimensionless parameter  $E't$ . Because these models work and can be correlated with actual open time measurements, the working theoretical model can be comfortably assumed valid. However, at this point it is unclear whether this treatment can be extended into pigmented systems or latexes thickened with rheology modifiers. This is an obvious extension of this study.

One of the key findings of this study is the fact that the relationship between the volume fraction occupied by the latex and weight fraction is anything but constant during the drying process. As a first approximation, the density of the polymer could be used to obtain  $V_f$ ; however, as clearly shown by the intrinsic viscosity data this assumption leads to a gross underestimation of this parameter. In some cases, the latex is more than twice the volume predicted from the density. Moreover, the data presented here shows that  $V_f$  is anything but constant during the drying process. This is not contrary to experience; however, the level of the effect is surprising. Factors such as neutralizing agent, initial pH, and cosolvent choice can have significant impact on the rheology during drying.

The effect that  $\text{NH}_4\text{OH}$  has on the viscosity of the drying film is very intriguing. In essence, our work shows that it is possible to prepare a latex sample which has a higher solid content and a higher pH than the control, and yet has a substantially lower viscosity. This effect can not be explained simply on the basis of the volatility of  $\text{NH}_4\text{OH}$  and the concomitant drop in pH. This means that the method by which a sample arrives at a given pH and weight-solids greatly impacts the viscosity. At this point we have no further insight into why the viscosity is suppressed in the  $\text{NH}_4\text{OH}$  samples, but we strongly

suspect that the effect is due to the contribution that  $\text{NH}_4^+$  has on shielding the double layer. In addition, we suspect that the macroscopically measured pH does not probe subtler effects that are happening on the latex surface.

## SUMMARY

The rheological changes during the initial stages of drying of a water-based latex film were examined for two lattices formulated at varying pH's with a variety of cosolvents, and different neutralizing agents. Water was found to evaporate from the films as if it were pure water with an activity coefficient of one and a heat of vaporization equivalent to pure water. The increase in viscosity during drying is explained by the volume packing models of Krieger and Dougherty or De Kruif. For several of the films in this study, the ratio between the volume and weight fractions was not a static parameter, and an abnormally large drop was observed in the effective volume occupied by the latex. This was exaggerated for the sample containing EB or  $\text{NH}_4\text{OH}$ . The former can be understood based on the high volatility of EB, while the latter effect indicates the surprising result, that  $\text{NH}_4\text{OH}$  substantially suppresses viscosity.

## ACKNOWLEDGMENT

The authors would like to thank Rohm and Haas for providing the funding for this work. We are also grateful for the contribution of R.P. Lauer and S.L. Tecce in synthesizing the latexes and measuring the accessible MAA in the latexes, and for the contribution of W. Thompson in measuring the cosolvent levels in the films. We are also grateful for the contribution of R.P. Lauer for help in editing this manuscript.

## References

- (1) (a) Rocklin, A.L., "Evaporation Phenomena: Precise Comparison of Solvent Evaporation Rates from Different Substrates," *JOURNAL OF COATINGS TECHNOLOGY*, 48, No. 622, 45 (1976); (b) Sullivan, D.A., "Water and Solvent Evaporation from Latex and Latex Paint Films," *JOURNAL OF PAINT TECHNOLOGY*, 47, No. 610, 60 (1975).
- (2) (a) Dillon, P.W., "Application of Critical Relative Humidity, An Evaporation Analog of Azeotropy, to the Drying of Waterborne Coatings," *JOURNAL OF COATINGS TECHNOLOGY*, 49, No. 634, 38 (1977); (b) Langmuir, I., *American Academy*, 2, 5, 329 (1913); (c) Knudsen, M., *Ann. Physik*, 47, 697 (1915); (d) Gardner, G.S., *Ind. Eng. Chem.*, 32, 2, 226 (1940); (e) Gilbert, T.E., "Rate of Evaporation of Liquids into Air," *JOURNAL OF PAINT TECHNOLOGY*, 43, No. 562, 93 (1971).
- (3) (a) Weinmann, K., *Farbe and Lack*, 10, 571 (1960); (b) Dillon, R.E., Matheson, L.A., and Bradford, E.B., *J. Colloid Sci.*, 6, 108 (1951); (c) Brown, G.L., *J. Polymer Sci.*, 22, 423 (1956); (d) Vanderhoff, J.W., *J. Makromol. Chem.*, 1, 361 (1966); (e) Voyutskii, S.S., *J. Polymer Sci.*, 32, 528 (1958); (f) Mleziva, P. and Milic, R., *Farbe and Lack*, 1, 9 (1989); (g) Kornum, L.O., *J. Oil & Colour Chemists' Assoc.*, 63, 3, 103 (1980); (h) McEwan, I.H., "Role of Water in Water-Reducible Paint Formulations," *JOURNAL OF PAINT TECHNOLOGY*, 45, 583, 33 (1973).
- (4) Dougherty, T.J. and Krieger, I., *Adv. Coll. Inter. Sci.*, 3, 111 (1972).
- (5) De Kruif, C.G., *J. Chem. and Phys.*, 83, 8, 4717 (1985).
- (6) Hansen, C.M., *Prog. Org. Coat.*, 11, 219 (1983).
- (7) Sletmo, G.M., "Evaporation of Nonhydrogen-Bonding Solvents from Resins Films," *JOURNAL OF PAINT TECHNOLOGY*, 38, No. 502, 641 (1966).
- (8) Doolittle, *Tech. of Solvents and Plasticizer*, Wiley, New York, 74, 1963.
- (9) Rasmussen, D.J., "Evaporation of Thinners and Solvents," *OFFICIAL Digest*, 27, No. 367, 529 (1955).
- (10) Saarly, Z. and Goff, P.L., "New Instrument to Measure Solvent Evaporation," *JOURNAL OF PAINT TECHNOLOGY*, 43, No. 583, 45 (1973).
- (11) Walsham, J.G. and Edwards, G.D., "A Model of Evaporation from Solvent Blends," *JOURNAL OF PAINT TECHNOLOGY*, 43, No. 554, 64 (1971).
- (12) Gilliland, E.R., *Ing. Eng. Chem.*, 26, 681, 1934.
- (13) Eaton, R.F. and Willeboordse, F.G., "Evaporation Behavior of Organic Cosolvents in Waterborne Formulations," *JOURNAL OF COATINGS TECHNOLOGY*, 52, No. 660, 63 (1980).
- (14) Krieger, I., *Adv. Coll. and Inter. Sci.*, 3, 111 (1972).
- (15) (a) Hansen, C.M., *Ing. Eng. Chem. Prod. Res. Rev.*, 16, 3, 266 (1977); (b) Hansen, C.M., *Ind. Eng. Chem. Prod. Res. Rev.*, 13, 2, 150 (1974).
- (16) Pramoganey, N.M., *S. Diss.*, Lehigh University, 1977.
- (17) Fox, T.G., *Bull. Am. Phys. Soc.*, 1, 123 (1956).

## Symbol list

T	.....	Absolute temperature
Emax	.....	Number of molecules evaporating out of the liquid
A	.....	Surface area of evaporating liquid
k	.....	Mass transfer factor
P <sub>v</sub>	.....	Vapor pressure of the evaporating liquid
M	.....	Molecular weight of the evaporating molecules
R	.....	Ideal gas constant
E <sub>L</sub>	.....	Absolute evaporation rate
D	.....	Diffusion coefficient of the evaporating gas molecules through the ambient gas
p	.....	Ambient pressure
x	.....	Effective boundary layer film thickness at the liquid surface
f	.....	Factor which is dependent on S
S	.....	Height of the stagnant air column above the liquid
Y	.....	Mean free path of the molecules in the vapor phase
dm/dt	.....	Evaporation rate
K <sup>v,T</sup>	.....	Mass transfer coefficient which depends on air flow (v) and temperature
p <sub>i</sub>	.....	Vapor pressure
a	.....	Activity coefficient
φ	.....	Relative vapor saturation (relative humidity)
C <sup>v,T</sup>	.....	Combination of temperature dependent factors from equation (4)
V	.....	Air speed over evaporating liquid
K <sub>0</sub>	.....	Mass transfer coefficient in the absence of air flow
α, β	.....	Correction factors for air flow
ΔH	.....	Enthalpy of vaporization for the solvent
η	.....	Viscosity of the dispersed lattices
η <sub>0</sub>	.....	Viscosity of the dispersing medium
η <sub>r</sub>	.....	Relative viscosity
φ <sub>v</sub>	.....	Volume fraction of dispersed latex
φ <sub>m</sub>	.....	Weight fraction of dispersed latex
P <sub>k</sub>	.....	Volume packing fraction
V <sub>f</sub>	.....	Ratio of volume to weight fraction of dispersed latex
V <sub>f</sub> (t)	.....	Time dependent ratio of the volume fraction to the weight fraction
V <sub>f</sub> <sup>1</sup>	.....	Ratio of volume to weight fraction of dispersed latex at low volume fractions
V <sub>f</sub> <sup>h</sup>	.....	Ratio of volume to weight fraction of dispersed latex at critical packing
E'	.....	Relative rate of evaporation (1/min)
m	.....	Initial mass of the film